Supported Catalytically-Active Supramolecular Hydrogels for Continuous Flow Chemistry

Jennifer Rodon Fores, Miryam Criado-Gonzalez, Alain Chaumont, Alain Carvalho, Christian Blanck, Marc Schmutz, Christophe Serra, Fouzia Boulmedais, Pierre Schaaf, Loïc Jierry

Supported Catalytically Active Supramolecular Hydrogels for Continuous Flow Chemistry

Jennifer Rodon Fores, Miryam Criado-Gonzalez, Alain Chaumont, Alain Carvalho, Christian Blanck, Marc Schmutz, Christophe A. Serra, F. Boulmedais, Pierre Schaaf, and Loïc Jierry**

Abstract: *Inspired by biology, one current goal in supramolecular chemistry is to control the emergence of new functionalities arising from the self-assembly of molecules. In particular, some peptides can self-assemble and generate exceptionally catalytically active fibrous networks able to underpin hydrogels. Unfortunately, the mechanical fragility of these materials is incompatible with process developments, relaying this exciting field to academic curiosity. Here, we show that this drawback can be circumvented by enzyme-assisted self-assembly of peptides initiated at the walls of a supporting porous material. We applied this strategy to grow an esterase-like catalytically active supramolecular hydrogel (CASH) in an open-cell polymer foam, filling the whole interior space. Our supported CASH material is highly efficient towards inactivated esters and enables the kinetic resolution of racemates. This hybrid material is robust enough to be used in continuous flow reactors, and is reusable and stable over months.*

One current goal in supramolecular chemistry is to control the emergence of new functionalities resulting from self-assembled organizations built by bottom-up approaches.[1,2] Recently, supramolecular hydrogels prepared by self-assembly of low molecular weight hydrogelators (LMWHs), mainly peptide derivatives, that exhibit catalytic properties were reported.[3,4] Based on the specific organization of peptide hydrogelators in nanofibers, the network displays enzyme-like features. Unfortunately, their catalytic activity used to be evaluated solely on model substrates. For instance, only very few studies have reported on supramolecular hydrogels displaying esterase activity on non-activated substrates. In addition, the use of catalytically active supramolecular hydrogels (CASHs) is not obvious: These reported hydrogels must first be vortexed to obtain a liquid solution of catalytic self-assembled fibers, complicating their separation from the product formed. Furthermore, when the process is based on a substrate solution diffusing into a CASH in order to let the chemical transformation take place within the gel, product isolation requires the entire CASH to be destructed. Last but not least, all CASH systems are not mechanically robust, restricting their handling and use in a chemical reactor.[5]

To render very soft materials such as hydrogels mechanically robust, the use of polymer foams as an internal skeleton that will rigidify the matter is an interesting approach.[6] In the case of peptide-based hydrogels, a first technological issue that needs to be resolved is the spatial localization of the hydrogel growth from the surface of the polymer foam in order to link the hydrogel and the polymer material. This can be achieved by immobilizing a (bio)catalyst on a planar surface.[7–10] We immobilized an enzyme that is able to transform non-self-assembling precursors present in solution into self-assembling building blocks on the surface.[11] The confinement of these building blocks at the material–water interface induces the growth of nanofibers anchored on the surface and underpinning the hydrogel.[12–14]

The development of a supported CASH is based on the appropriate choice of precursor, which has to fulfill two essential requirements: It must 1) generate self-assembling derivatives in the presence of an adequate enzyme and 2) result in a supramolecular hydrogel exhibiting catalytic activity. Up to now, no such LMWH precursors have been described. Among the catalytically active supramolecular hydrogels reported in the literature,[15] our attention focused on the peptide sequence *Nap*-GFFYGHY (*Nap* = naphthalene) described by Yang and co-workers.[16] This peptide is not soluble in water at room temperature but when a suspension of this peptide is heated close to 100 °C and then cooled slowly, an esterase-like hydrogel is obtained that is reactive towards the activated ester 4-nitrophenyl acetate (PNA). The

[*] J. Rodon Fores, Dr. M. Criado-Gonzalez, A. Carvalho, C. Blanck, Dr. M. Schmutz, Prof. Dr. C. A. Serra, Dr. F. Boulmedais, Prof. Dr. P. Schaaf, Prof. Dr. L. Jierry
Université de Strasbourg, CNRS
Institut Charles Sadron (UPR22)
23 rue du Loess, BP 84047, 67034 Strasbourg Cedex 2 (France)
E-mail: schaaf@unistra.fr
loic.jierry@ics-cnrs.unistra.fr
Dr. M. Criado-Gonzalez, Prof. Dr. P. Schaaf
Institut National de la Santé et de la Recherche Médicale
INSERM Unité 1121
11 rue Humann, 67085 Strasbourg Cedex (France),
and
Université de Strasbourg
Faculté de Chirurgie Dentaire
8 rue Sainte Elisabeth 67000 Strasbourg (France)
Dr. A. Chaumont
Université de Strasbourg
Faculté de Chimie, UMR7140
1 rue Blaise Pascal, 67008 Strasbourg Cedex (France)

most interesting aspect of this heptapeptide regarding our goal lies in the presence of two tyrosine residues (Y) in positions 4 and 7: Phosphorylation of the two phenol groups was necessary to obtain a bis-phosphorylated heptapeptide Fmoc-GFF*p*YGH*p*Y (Figure 1 a) well soluble in water (see the Supporting Information, Section S2).

When alkaline phosphatase (AP) is added to a 1 mol % solution of Fmoc-GFF*p*YGH*p*Y, a quasi-translucent hydrogel forms almost instantaneously (Figure 1 b) consisting to 97 % of the twice dephosphorylated Fmoc-GFFYGHY (Figure S1). The resulting peptide produced enzymatically in situ leads to entangled, several-micrometer-long fibers observable by transmission electron microscopy (TEM) (Figure 1 c). Magnification of the image of these fibers suggests

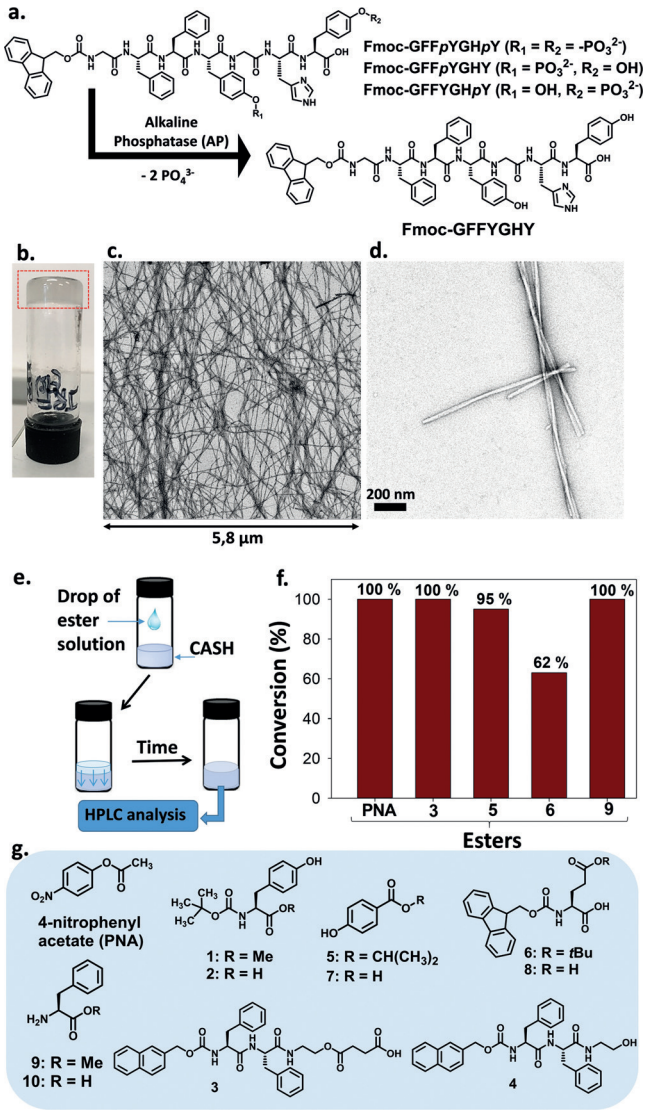

Figure 1. a) Enzymatic transformation of Fmoc-GFF*p*YGH*p*Y in Fmoc-GFFYGHY. b) Upside down vial containing the Fmoc-GFFYGHY hydrogel. c) TEM image of Fmoc-GFFYGHY self-assembled nanofibers. d) Magnification of the TEM image. e) Schematic representation of the process based on the diffusion of the ester substrates within the CASH. f) Conversion of ester substrates PNA, **3**, **5**, **6**, and **9**. g) Ester substrates and their corresponding carboxylic acids.

a ribbon shape with a width of 27 nm and a right-handed twist with a pitch of approximately 300 nm when two or more ribbons are associated together (Figure 1 d). The CD spectrum is consistent with a β-sheet structure, in agreement with literature reports on similar peptide assemblies.[17] IR spectroscopy confirmed that roughly 66 % of β-sheets are in the structure.[18,19] A rheological study of this CASH hydrogel provided G′ and G″ values of 3.6 kPa and 0.3 kPa, respectively, at 0.3 Hz (Section 20). The hydrogelation process takes place in less than one minute. Below a strain value of 6 %, the supramolecular network behaves as a gel whereas above this strain, it becomes liquid-like. When the hydrogel is put in contact with a PNA solution (1 mM) as depicted in Figure 1 e (Section 14), the gel spontaneously turns yellow because of *para*-nitrophenol production (Figure S3). However, this way of producing carboxylic acid derivatives is not practical: Aside from the mechanical fragility of such supramolecular hydrogels, the time required for the substrate to penetrate the CASH and the time required to reach full conversion (because of the substrate diffusion inside the hydrogel) are long. More importantly, the isolation of the formed carboxylic acid derivatives requires the dissolution of the CASH followed by purification steps, sentencing this self-assembled catalytic material to a single run. Therefore, this way to realize the catalytic reaction is time-consuming, expensive, and tedious, motivating our investigations of supported CASH systems.

To build our supported CASH, we used a commercial open-cell melamine foam with cell diameters of about 200 µm as the porous catalyst support (Figure 2 a). The foam was designed to achieve a suitable tubular shape and placed inside a metallic column as shown in Figure 2 b (length: 15 cm; diameter: 4 mm). On the walls of the pores, we deposited a polyelectrolyte multilayer consisting of 2.5 PEI/PSS bilayers (PEI = poly(ethylene imine), PSS = poly(styrene sulfonate)) covered by an AP layer by dipping alternately in PEI, PSS, and AP solutions (Figure 2 c). We then passed an Fmoc-GFF*p*YGH*p*Y solution through the functionalized column to form the supported CASH (Section 16). Cryo-SEM (at low etching) analysis of this coated foam showed that the supported CASH is filling the whole space of the polymer foam (Figure 2 d).

To further characterize the supported CASH, and because the use of multiple layers renders the buildup process independent of the substrate, we investigated it on flat surfaces where more characterization techniques are available. We modified the surfaces with an enzymatically active multilayer similar to that deposited on the foam walls. The buildup of the multilayer was first monitored by quartz crystal microbalance with dissipation (QCM-D) analysis and found to generate a 19 nm thick $(PEI/PSS)_2/PEI/AP$ film (Section S5). When this so-modified substrate was brought in contact with Fmoc-GFF*p*YGH*p*Y solution, a huge decrease in all QCM frequencies was observed, characteristic of highly hydrated mass deposition. This decrease continued more slowly over 12 h without levelling off, suggesting a continuing gelation process over this period of time (Figure S4).[13,14] AFM, SEM, HPLC composition analysis, and fluorescence emission intensity measurements confirmed the nanofibrous

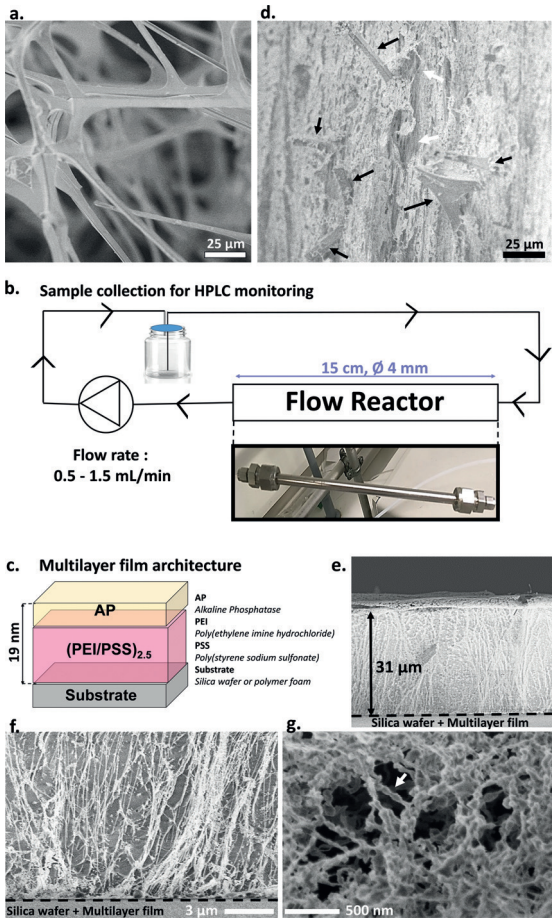

Figure 2. a) Melamine open cell foam observed by SEM. b) Continuous flow reactor. c) Multilayer film architecture. d) Z-section view of a CASH supported on a melamine open cell foam observed by cryo-SEM. Black arrows indicate the backbone of the polymer foam. White arrows show the fibrous network located everywhere within the interior space of the hydrogel-filled foam. e) Cryo-SEM image of the CASH formed on a silica wafer. f) Magnification of the substrate/CASH interface. g) Magnification of the helical nanofibers (white arrow).

architecture of the hydrogel made up of the hydrogelator Fmoc-GFFYGHY with Fmoc groups stacking together through π–π interactions in the resulting assembly (Figures S5–S7).[13,17] Cryo-SEM analysis was realized on CASH grown up from a silica wafer. The sample was cut in the *z*-section in order to measure the thickness of the formed hydrogel when the substrate was in contact with the Fmoc-GFF*p*YGH*p*Y solution for 12 h. The CASH thickness is roughly 31 µm, a regular value all along the sample (Figure 2e). Strikingly, we noticed a perpendicular orientation of the fibers starting from the surface, as already observed:[20] a fibrous architecture different from what is observed when the hydrogel is formed in the bulk. Some of the fibers collapsed but thinner fibers were also present (Figure 2f). As observed by TEM, these nanofibers seem to have a chiral twisted ribbon shape (Figure 2g). Complete ester hydrolysis was observed in a few minutes when this silica-wafer-supported hydrogel layer was dipped into PNA solution (Section S14 and Figure S8).

The catalytic activity of this supported CASH in a flow reactor was first evaluated using PNA as the substrate at 1 mM with 1.5 mL min^{-1} as the flow rate: After 2.8 min, the hydrolysis conversion amounted to 98%. This duration corresponds to the cumulative residence time of the substrate in the supported CASH column in a closed-loop system. The flow in such a reactor, where the substrate flows through a porous material, follows a plug flow.[21] HPLC analysis also confirmed that no constituting peptide hydrogel, that is, Fmoc-GFFYGHY, was released from the column, suggesting the preservation of its integrity during the catalytic process. Five successive runs were realized under identical conditions without loss of catalytic efficiency, highlighting the effective recycling of the supported CASH. Remarkably, this catalytic reactor can be stored (4 °C) for at least one month and reused again without a decrease in activity (Figure S9). As the catalytic properties result from the peptide self-assembly, this repeatability highlights the robustness of the nanofibrous network under flow conditions. Moreover, we have also shown that the applied flow rate, which was varied over two orders of magnitude, does not affect the conversion for a fixed residence time of the substrate. This is one more piece of evidence that the self-assembled architecture is not affected by the flow under our conditions (Figure S10). We also confirmed that the catalytic activity is independent of the location along the tubular reactor (Figure S11), showing that the catalytic hydrogel formed along the porous support is homogeneously distributed all over the tubular foam. Using concentrations of PNA lower than 2.20 mM led to full ester hydrolysis, and thus 2.20 mM of *para*-nitrophenol was generated. However, when higher concentrations of PNA were used (2.78, 8.20, 10, 22, or 41 mM), only 141 ± 7 µmoles of PNA were transformed into *para*-nitrophenol, corresponding to conversions of 99, 52, 49, 24, and 17%, respectively (Figure 3a). This result suggests that PNA poisons the catalytic self-assembly when high concentrations of this substrate are used. Actually, *para*-nitrophenyl esters are well-known to be powerful acylating agents toward imidazole groups.[22] With a non-acylating substrate such as methyl ester **1**, complete hydrolysis was observed irrespective of its concentration: 1.0, 2.2, 8.2, 22.0, or 41.0 mM (Figure 3c). As one PNA molecule can acylate only one imidazole group, it is possible to calculate the number of histidine residues involved in the catalytic pocket: We thus determined that one of eleven peptides is involved in the catalytic self-assembly (Section S17). However, the acylation of imidazole is a reversible reaction and washing the column with adequate amounts of water entirely restores its initial catalytic activity (Figure S12).[23]

Molecular dynamics show the spatial organization of 16 Fmoc-GFFYGHY (Figures 3b and S13 and Section 19) calculated from an initial random distribution state of all peptides in a cubic simulation box (edge: 5.2 nm). After equilibration, the system was let to evolve during 50 µs. Fmoc groups are stacked together through π–π interactions with distances from approximately 3.97 to 5.10 Å (Figure S13). Interestingly, two pairs of histidine residues linked together through hydrogen bonding appear in Figure 3b. The organization of two histidine residues allows cooperative actions,

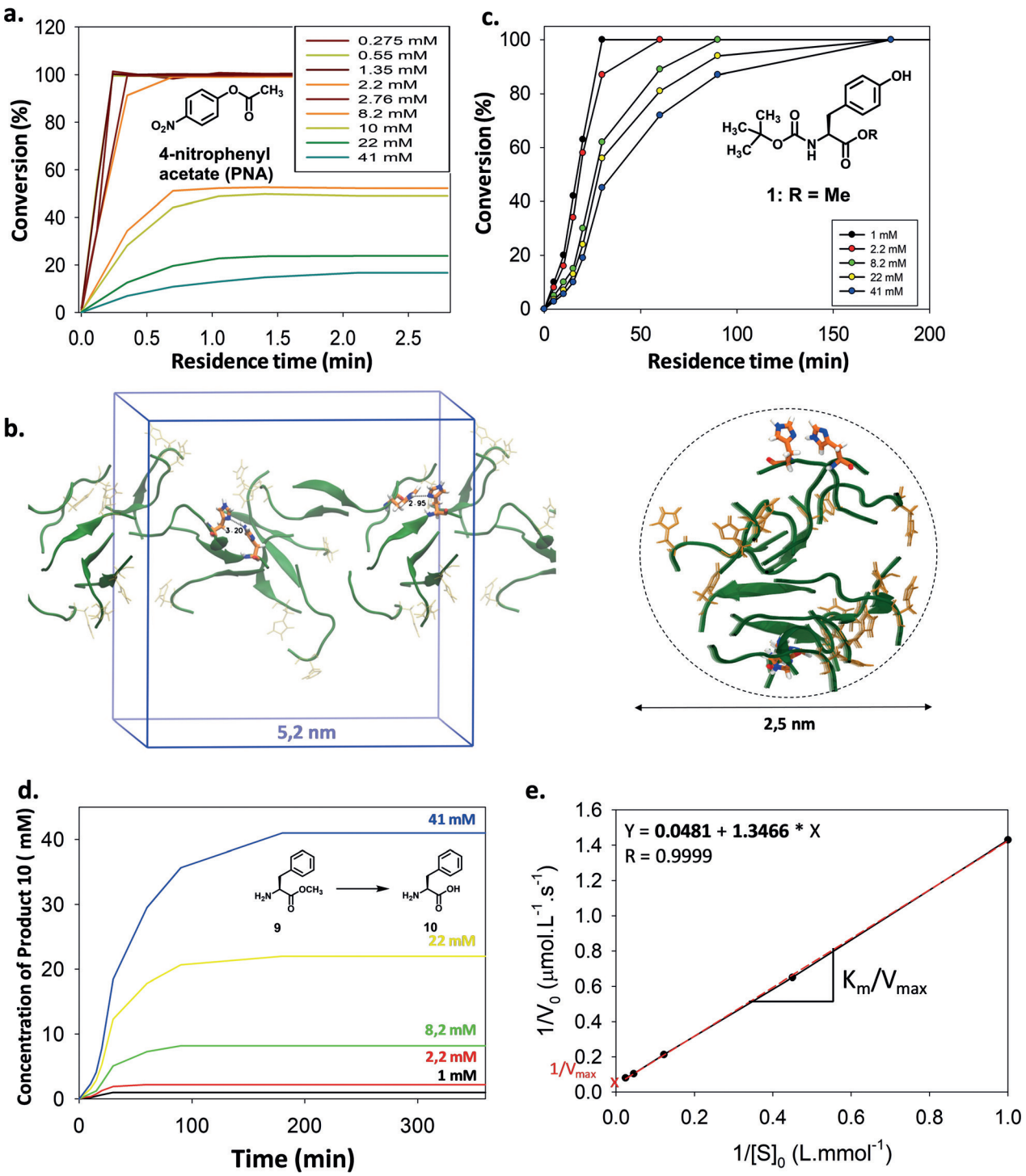

Figure 3. a) PNA conversion over time. b) Left: Molecular dynamics of 16 peptides Fmoc-GFFYGHY showing a fiber-like spatial arrangement. (The blue square represents the unit cubic simulation box to which 3D periodic boundary conditions were applied. Fmoc groups are not shown for clarity.) Right: The fiber diameter is 2.5 nm. Two pairs of histidine residues linked together through hydrogel bonding are bolded and shown in orange (others histidine are shown in light yellow). c) Hydrolysis conversion of ester **1** over time. d) Production of acid **10** over time from ester **9**. e) Determination of V_{max} and K_m values according to the Lineweaver–Burk model (linear regression as a dashed red line).

leading to amplified catalytic properties. The histidine residue is directly involved in the esterase activity of the assembly where the pK_a value of the imidazole group plays a crucial role in the catalytic efficiency. The pK_a value of the imidazole group in a histidine residue is 6.8 but it is known that the environment can have an impact on this value.[24] The pK_a value of the imidazole moiety of the peptide Fmoc-GFFY-GHY in the self-assembled state was determined to be 5.4 ± 0.5 (Section S21). This indicates an increase in basicity of the imidazole groups that is due to the environment created by

the self-assembly. The diameter of this simulated fiber-like structure is lower than that measured on the fibers observed by TEM (Figure 1d). It can be expected that lateral interactions between fiber-like structures may result in nanofibril organization.

Interestingly, we discovered that this CASH is also highly effective in the hydrolysis of a wide range of inactivated esters, which is rarely reported, when the substrate has diffused into the catalytic hydrogel (Figure 1g). Tertiary esters such as **6** require more time to be fully hydrolyzed (Figure S14), and complex structures such as **3** can self-assemble when the ester moiety is chemically cleaved,[25] giving rise to a second self-assembled architecture growing within the CASH (Figure S15).[26] This substrate versatility is crucial with regard to developments for chemical synthesis tools. Using a flow reactor, the hydrolysis reaction is fast (Figure S16). For instance, the inactivated methyl ester **1** (1 mM) is entirely hydrolyzed into **2** in less than 40 min (25 °C, 1.5 mL min^{-1}). Increasing the concentration of **1** extends the necessary residence time but without inhibition effects, as expected for this non-acylating substrate (Figure 3c). A linear dependence of $1/V_0$ on 1/[S], where V_0 is the initial reaction rate and [S] is the concentration of substrate **9** (Figure 3d and Section S18), was observed, showing the Michaelis–Menten behavior of our enzyme-like supported CASH (Figure S17). We also determined the following values: $K_m = 28$ mM, $V_{max} = 20.8$ μmol s^{-1}, and $k_{cat} = 3.0 \times 10^3$ s^{-1}. This k_{cat} value is at least ten times higher than those reported for other CASH systems with activated *para*-nitrophenol ester derivatives.[27,28]

In the literature, there are only few CASH-enabled enantioselective processes,[29,30] and the kinetic resolution of inactivated esters by CASH is still an unsolved challenge.[15,27,31] We observed strong discrimination by the supported CASH between L- and D-amino acid *tert*-butyl esters **6**: indeed, after a residence time of 30 min, we observed that almost 45% of the natural enantiomer L-**6** had been hydrolyzed whereas D-**6** had not been yet affected (Figure 4a). By decreasing the flow rate to 0.5 mL min^{-1}, it was possible to achieve more than 90% conversion of L-**6** into its corresponding acid derivative L-**8** (Figure 4b). After loading the flow reactor with 200 mg of racemic *rac*-**6** and using a flow rate of 0.5 mL min^{-1}, we stopped the reaction after 30 min. The reaction medium was slightly basified and extracted with dichloromethane, yielding chemically pure acid L-**8** as a white solid in 95% yield with 99% enantiomeric excess (*ee*) from the aqueous phase (Figure 4b and inset). The non-hydrolyzed ester D-**6** was isolated with a chemical yield of 96% and 92% *ee* from the organic layer. Enantioenriched L-**6** (40% *ee*) lead quasi-quantitative isolation of both enantiopure L-**8** and the ester D-**6** (Figure S18). Racemic *tert*-butyl esters of other amino acids such as lysine and tyrosine were also tested: In both cases, we observed faster hydrolysis of the L-enantiomer (Figure S20), highlighting the ability of the catalytic pocket to react faster with the natural amino acids. Finally, other racemic esters were tested such as the oxirane of 4-methoxycinnamic methyl ester, where the *R*,*R* enantiomer was hydrolyzed faster than the *S*,*S* enantiomer (Figure S19). This compound is a key intermediate in the industrial preparation

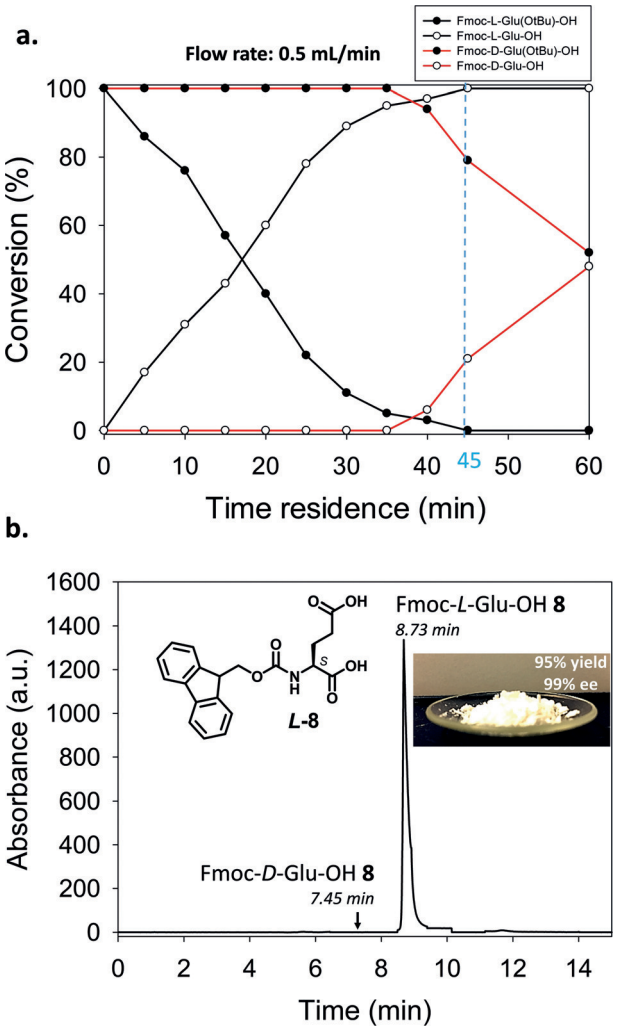

Figure 4. a) Amount of L-**6** and D-**6** and their corresponding hydrolyzed derivatives L-**8** and D-**8** over time at a flow rate of 0.5 mL min^{-1}. b) Determination of the *ee* of isolated L-**8** by HPLC analysis on a chiral stationary phase and photograph of chemically and enantiomerically pure L-**8** obtained by using the supported CASH system in a continuous flow process.

of diltiazem, a drug used to treat high blood pressures, angina, and certain heart arrhythmias.

Continuous flow chemistry appears to be particularly well adapted for CASH applications as the flow through the catalytic hydrogel compensates the low diffusion rate of substrates under static conditions (thus decreasing the reaction time) and provides an easy method to separate the products from the catalytic phase. These features were not obvious because supramolecular hydrogels are physical gels resulting from the self-assembly of small molecules and thus a gradual delamination of the CASH through the shear stress induced by the flow is a scenario that was not possible to rule out at first sight.

Yet supported CASH systems proved to be stable with respect to flow and over time, and the catalytic process could be repeated several times without any loss of activity. Our designed supported CASH gives rise to an efficient esterase-like hydrogel active towards activated esters but also towards

a large panel of inactivated substrates such as methyl, primary, secondary, and tertiary esters, a feature never reported before. Last but not least, our supported CASH also shows kinetic resolution capacity, enabling the isolation of quantitative amounts of enantiopure carboxylic acids from racemic or enantioenriched inactivated esters. The precise tuning of the molecular assembly, directing the emergence of functional nanostructures through a bottom-up approach and leading to highly functional materials, is a new concept recently introduced by Ariga and co-workers.[32,33] In our work, we have shown that the spatial control of peptide self-assembly from the surface of porous polymer materials leads to the growth of nanofibrous networks. From this nano-organization catalytic properties arise, allowing the design of a functional material for applications in flow chemistry. We thus highlight that the supported CASH can be a powerful tool for the design of new nanoarchitectures and can find applications in various areas of chemistry, from synthetic chemistry to materials science and chemical engineering.[34]

Acknowledgements

This work was financially supported by the Agence Nationale de la Recherche (project "EASA" ANR-18-CE06-0025-03, "POLYCATPUF" ANR-16-CE07-0030-01, and "MECHANOCAT" ANR-15-CE29-015), the Fondation pour la Recherche en Chimie (project number PSC-005), the Labex Chimie des Systèmes Complexes, and Institut Carnot-MICA (project *POLYSPRAY*). J.R.F. acknowledges the International Center for Frontier Research in Chemistry (Labex CSC, project number PSC-016) for a PhD fellowship. The ICS microscopy platform and the ICS characterization platform are acknowledged. We thank Alexandre Collard for his technical help in the setup of the flow reactor.

Conflict of interest

The authors declare no conflict of interest.

Keywords: hydrogels · kinetic resolution · organocatalysis · self-assembly · supported catalysis

[1] J.-M. Lehn, *Angew. Chem. Int. Ed.* **2015**, *54*, 3276 – 3289; *Angew. Chem.* **2015**, *127*, 3326 – 3340.
[2] G. M. Whitesides, B. Grzybowski, *Science* **2002**, *295*, 2418 – 2421.
[3] M. O. Guler, S. I. Stupp, *J. Am. Chem. Soc.* **2007**, *129*, 12082 – 12083.
[4] F. Rodríguez-Llansola, B. Escuder, J.-F. Miravet, *J. Am. Chem. Soc.* **2009**, *131*, 11478 – 11484.
[5] R. G. Weiss, *J. Am. Chem. Soc.* **2014**, *136*, 7519 – 7530.
[6] N. Teramoto, O. Shigehiro, Y. Ogawa, Y. Maruyama, T. Shimasaki, M. Shibata, *Polym. J.* **2014**, *46*, 592 – 597.
[7] A. G. L. Olive, N. H. Abdullah, I. Ziemecka, E. Mendes, R. Eelkema, J. H. van Esch, *Angew. Chem. Int. Ed.* **2014**, *53*, 4132 – 4136; *Angew. Chem.* **2014**, *126*, 4216 – 4220.
[8] X. Du, J. Zhou, J. Shi, B. Xu, *Chem. Rev.* **2015**, *115*, 13165 – 13307.
[9] C. Vigier-Carrière, F. Boulmedais, P. Schaaf, L. Jierry, *Angew. Chem. Int. Ed.* **2018**, *57*, 1448 – 1456; *Angew. Chem.* **2018**, *130*, 1462 – 1471.
[10] B. Yang, D. J. Adams, M. Marlow, M. Zelzer, *Langmuir* **2018**, *34*, 15109 – 15125.
[11] Z. Yang, H. Gu, D. Fu, P. Gao, J. K. Lam, B. Xu, *Adv. Mater.* **2004**, *16*, 1440 – 1444.
[12] R. J. Williams, A. M. Smith, R. Collins, N. Hodson, A. K. Das, R. V. Ulijn, *Nat. Nanotechnol.* **2009**, *4*, 19 – 24.
[13] C. Vigier-Carrière, T. Garnier, D. Wagner, P. Lavalle, M. Rabineau, J. Hemmerlé, B. Senger, P. Schaaf, F. Boulmedais, L. Jierry, *Angew. Chem. Int. Ed.* **2015**, *54*, 10198 – 10201; *Angew. Chem.* **2015**, *127*, 10336 – 10339.
[14] J. Rodon Fores, M. L. M. Mendez, X. Mao, D. Wagner, M. Schmutz, M. Rabineau, P. Lavalle, P. Schaaf, F. Boulmedais, L. Jierry, *Angew. Chem. Int. Ed.* **2017**, *56*, 15984 – 15988; *Angew. Chem.* **2017**, *129*, 16200 – 16204.
[15] O. Zozulia, M. A. Dolan, I. V. Korendovych, *Chem. Soc. Rev.* **2018**, *47*, 3621 – 3639.
[16] C. Yang, H. Wang, D. Li, L. Wang, *Chin. J. Chem.* **2013**, *31*, 494 – 500.
[17] A. M. Smith, R. J. Williams, C. Tang, P. Coppo, R. F. Collins, M. L. Turner, A. Saiani, R. V. Ulijn, *Adv. Mater.* **2008**, *20*, 37 – 41.
[18] N. Yamada, K. Ariga, M. Naito, K. Matsubara, E. Koyama, *J. Am. Chem. Soc.* **1998**, *120*, 12192 – 12199.
[19] S. Fleming, P. W. J. M. Frederix, I. R. Sasselli, N. T. Hunt, R. V. Ulijn, T. Tuttle, *Langmuir* **2013**, *29*, 9510 – 9515.
[20] M. Reches, E. Gazit, *Nat. Nanotechnol.* **2006**, *1*, 195 – 200.
[21] H. Scott Fogler, *Elements of Chemical Reaction Engineering*, 3rd ed., Prentice Hall, Upper Saddle River, **1999**.
[22] M. L. Bender, B. W. Turnquest, *J. Am. Chem. Soc.* **1957**, *79*, 1652 – 1655.
[23] Y. S. Moroz, T. T. Dunston, O. V. Makhlynets, O. V. Moroz, Y. Wu, J. H. Yoon, A. B. Olsen, J. M. McLaughlin, K. L. Mack, P. M. Gosavi, N. A. J. van Nuland, I. V. Korendovych, *J. Am. Chem. Soc.* **2015**, *137*, 14905 – 14911.
[24] K. Ariga, T. Nakanishi, J. P. Hill, M. Shirai, M. Okuno, T. Abe, *J. Am. Chem. Soc.* **2005**, *127*, 12074 – 12080.
[25] J. Li, Y. Kuang, J. Shi, J. Zhou, J. E. Medina, R. Zhou, D. Yuan, C. Yang, H. Wang, Z. Yang, J. Liu, D. M. Dinulescu, B. Xu, *Angew. Chem. Int. Ed.* **2015**, *54*, 13307 – 13311; *Angew. Chem.* **2015**, *127*, 13505 – 13509.
[26] N. Singh, C. Maity, K. Zhang, C. A. Angulo-Pachon, J. H. van Esch, R. Eelkema, B. Escuder, *Chem. Eur. J.* **2017**, *23*, 2018 – 2021.
[27] N. Singh, M. P. Conte, R. V. Ulijn, J. F. Miravet, B. Escuder, *Chem. Commun.* **2015**, *51*, 13213 – 13216.
[28] K. L. Duncan, R. V. Ulijn, *Biocatalysis* **2015**, *1*, 67 – 81.
[29] F. Rodríguez-Llansola, J. F. Miravet, B. Escuder, *Chem. Commun.* **2009**, 7303 – 7305.
[30] N. Singh, K. Zhang, C. A. Angulo-Pachon, E. Mendes, J. H. van Esch, B. Escuder, *Chem. Sci.* **2016**, *7*, 5568 – 5572.
[31] A. Som, S. Matile, *Eur. J. Org. Chem.* **2002**, 3874 – 3883.
[32] M. Aono, K. Ariga, *Adv. Mater.* **2016**, *28*, 989 – 992.
[33] M. Komiyama, K. Yoshimoto, M. Sisido, K. Ariga, *Bull. Chem. Soc. Jpn.* **2017**, *90*, 967 – 1004.
[34] L. Zhao, Q. Zou, X. Yan, *Bull. Chem. Soc. Jpn.* **2019**, *92*, 70 – 79.